bioRxiv preprint doi: https://doi.org/10.1101/2022.01.05.475171; this version posted January 7, 2022. The copyright holder for this preprint (which was not certified by peer review) is the author/funder, who has granted bioRxiv a license to display the preprint in perpetuity. It is made available under aCC-BY-ND 4.0 International license.

The diversity and functional capacity of microbes associated with coastal phototrophs

Khashiff Miranda[1,2*], Brooke L. Weigel[3,4], Emily C. Fogarty[5,6], Iva A. Veseli[7], Anne E. Giblin[8], A. Murat Eren[5,9], Catherine A. Pfister[3,10]

[*] Corresponding author email: khashiff.miranda.1@ulaval.ca

[1] The College, The University of Chicago, Chicago, IL, 60637, USA

[2] Département de biologie, Université Laval, Québec, QC, G1V 0A6, Canada

[3] Committee on Evolutionary Biology, The University of Chicago, Chicago, IL, 60637, USA

[4] Friday Harbor Laboratories, University of Washington, Friday Harbor, WA 98250, USA

[5] Department of Medicine, The University of Chicago, Chicago, IL 60637, USA

[6] Committee on Microbiology, The University of Chicago, Chicago, IL 60637, USA

[7] Biophysical Sciences Program, The University of Chicago, Chicago, IL, 60637, USA

[8] The Ecosystems Center, The Marine Biological Laboratory, Woods Hole, MA, 02543, USA

[9] Josephine Bay Paul Center, Marine Biological Laboratory, Woods Hole, MA 02543, USA

[10] Department of Ecology & Evolution, The University of Chicago, Chicago, IL, 60637 USA

Abstract

Coastal marine phototrophs exhibit some of the highest rates of primary productivity in the world. They have been found to host a diverse set of microbes, many of which may impact the biology of their phototroph hosts through metabolisms that are unique to microbial taxa. Here we characterized the metabolic functions of phototroph-associated microbial communities using metagenomes collected from 2 species of kelp (*Laminaria setchellii* and *Nereocystis luetkeana*)

bioRxiv preprint doi: https://doi.org/10.1101/2022.01.05.475171; this version posted January 7, 2022. The copyright holder for this preprint (which was not certified by peer review) is the author/funder, who has granted bioRxiv a license to display the preprint in perpetuity. It is made available under aCC-BY-ND 4.0 International license.

and 3 marine angiosperms (*Phyllospadix scouleri*, *P. serrulatus* and *Zostera marina*), including the rhizomes of two surfgrass species (*Phyllospadix* spp.) and the seagrass *Zostera marina*, and the sediments surrounding *P. scouleri* and *Z. marina*. Using metagenomic sequencing, we describe 72 metagenome assembled genomes (MAGs) that potentially benefit from being associated with macrophytes and may contribute to macrophyte fitness through their metabolic gene content. All host-associated metagenomes contained genes for the use of dissolved organic matter from hosts and vitamin (B_1, B_2, B_7, B_{12}) biosynthesis. Additionally, we found a range of nitrogen metabolism genes that transform dissolved inorganic nitrogen into forms that may be more available to the host. The rhizosphere of surfgrass and seagrass contained genes for anaerobic microbial metabolisms, including *nifH* genes associated with nitrogen fixation, despite residing in a well-mixed and oxygenated environment. The range of oxygen environments engineered by macrophytes likely explains the diversity of both oxidizing and reducing microbial metabolisms, and contributes to the functional capabilities of microbes and their influence on carbon and nitrogen cycling in nearshore ecosystems.

Importance

Kelps, seagrasses and surfgrasses are ecosystem engineers on rocky shorelines where they show remarkably high levels of primary production. Through analysis of their associated microbial communities, we found a variety of microbial metabolisms that may benefit the host, including nitrogen metabolisms and the production of B vitamins. In turn, these microbes have the genetic capability to assimilate the dissolved organic compounds released by their phototroph hosts. We describe a range of oxygen environments associated with surfgrass, including low-oxygen microhabitats in their rhizomes that host genes for nitrogen fixation. The tremendous

bioRxiv preprint doi: https://doi.org/10.1101/2022.01.05.475171; this version posted January 7, 2022. The copyright holder for this preprint (which was not certified by peer review) is the author/funder, who has granted bioRxiv a license to display the preprint in perpetuity. It is made available under aCC-BY-ND 4.0 International license.

47 productivity of coastal phototrophs is likely due in part to the activities of associated microbes
48 and an increased understanding of these associations is needed.
49

50 **Introduction**

51 We are experiencing a paradigm shift in biology with the recognition that many species exist as a
52 consortium with microbes (1). These microbial associations are nearly ubiquitous, spanning a
53 diversity of hosts across ecosystems. In coastal marine environments, phototrophic microbial
54 hosts are diverse and range from marine angiosperms to large eukaryotic protists (macroalgae).
55 Different macroalgal host species (2, 3) and different phototroph tissues (4, 5) host distinct
56 microbial communities numbering in the millions per cm^2 of host tissue (6), yet we still know
57 little about the functional role the microbiome plays in host fitness or how the host influences the
58 microbiome. The microbiome of phototroph species has been shown to have metabolisms that
59 provide nitrogen to the host (7, 8). Bacteria also supply B vitamins (9) and affect development of
60 their host (10). Further, the contributions that marine phototrophs make to host carbon and
61 nitrogen cycling have largely ignored the role that microbes play. Even as we begin to describe
62 their microbiome, we are discovering that environmental change affects these communities (11).
63 For many of the foundational phototrophic species in the coastal ocean, our understanding of the
64 diversity and role of their microbiome is nascent.
65

66 A unique aspect of host-associated microbes are the strong gradients in oxygen that they
67 experience due to the biological activities of the host. The photosynthetic and respiratory
68 activities of the host can generate a 'phycosphere' (12) where the host influences the physical
69 environment experienced by microbes, sometimes over micron or mm scales. For example, the

bioRxiv preprint doi: https://doi.org/10.1101/2022.01.05.475171; this version posted January 7, 2022. The copyright holder for this preprint (which was not certified by peer review) is the author/funder, who has granted bioRxiv a license to display the preprint in perpetuity. It is made available under aCC-BY-ND 4.0 International license.

basal leaf meristem of the seagrass *Zostera* ranges from oxic to anoxic conditions over a scale of 300 microns when measured with oxygen microsensors (13). This range of oxygen concentrations likely selects for a diversity of microbial metabolisms in association with macrophytes.

Another factor important to the microbial metabolisms associated with coastal macrophytes is nutrient availability. In coastal systems, nitrogen can limit primary production and microbial associates that aid in accessing nitrogen might be selected. Microbial metabolisms that can increase the available dissolved inorganic nitrogen (DIN) for the host (14) include pathways that cleave carbon-nitrogen bonds to generate ammonium. This ammonification in biological systems can result from a diversity of hydrolases, including ureases and other enzymes that cleave C-N bonds (15). Further, microbes that fix atmospheric nitrogen have been discovered in an increasing number of taxa (8, 16), now recognized to include heterotrophic as well as phototrophic taxa (17–19). Nitrogen fixation was previously assumed to be restricted to nitrogen-poor environments, but has been quantified recently in systems thought to be nitrogen-rich (8, 20), an enigmatic finding given that nitrogen fixation is a costly metabolic process that consumes 16 ATPs per N_2 fixed (21). Sediments where oxygen is low and nutrients can be depleted by macrophytes, such as the rhizosphere of seagrasses have provided evidence of nitrogen fixation (22–26). The recent discovery that nitrogen fixation takes place on particles in the coastal ocean where nitrate is relatively abundant (8, 20) suggests that *nifH* genes could be abundant in other nearshore systems.

bioRxiv preprint doi: https://doi.org/10.1101/2022.01.05.475171; this version posted January 7, 2022. The copyright holder for this preprint (which was not certified by peer review) is the author/funder, who has granted bioRxiv a license to display the preprint in perpetuity. It is made available under aCC-BY-ND 4.0 International license.

Microbial metabolisms that synthesize compounds and vitamins needed by seaweeds and seagrasses may also underlie host-microbe exchanges. The active form of Vitamin B1 (thiamin) is essential for all organisms and is involved in carbohydrate and amino acid metabolisms. Vitamin B2 (riboflavin)-binding proteins are co-enzymes in various oxidases and are involved in photosynthesis and phototropism (27). Vitamin B7 (biotin) is a cofactor for acetyl coenzyme A (coA) which is essential for fatty acid synthesis. Vitamin B12 (cobalamin) is required as a coenzyme in the mitochondria for many algae, yet they depend upon prokaryotes to produce it (9, 28). Thus, marine macrophytes may be auxotrophic for key vitamins, and their production by host-associated bacteria may be another basis for phototroph-microbiome interactions in nature.

Hosts might reciprocally benefit microbes, especially if heterotrophic microbes benefit from the dissolved organic carbon that is released by their hosts. Of the carbon that is fixed, kelp have been demonstrated to release 15-16% of it as dissolved organic matter (29, 30), and seagrasses too provide a constant source of dissolved organic carbon (31, 32), likely stimulating heterotrophic bacterial processes (33). These rates of organic carbon release, often involving highly labile organic carbon compounds (34), could provide the basis for reciprocal benefits between microbes and their associated hosts.

Here, we analyzed microbial metagenomes collected from 5 different coastal phototrophs to determine if there is functional genomic evidence of microbial metabolisms that could reciprocally benefit host and microbes. We analyzed the surface microbiome on the blade of two kelp species (*Laminaria setchellii* and *Nereocystis luetkeana*) and the surfgrass *Phyllospadix scouleri*, the rhizomes of *P. scouleri, P. serrulatus*, and the seagrass species, *Zostera marina,* and

bioRxiv preprint doi: https://doi.org/10.1101/2022.01.05.475171; this version posted January 7, 2022. The copyright holder for this preprint (which was not certified by peer review) is the author/funder, who has granted bioRxiv a license to display the preprint in perpetuity. It is made available under aCC-BY-ND 4.0 International license.

the sediment surrounding the rhizomes of *P. scouleri* and *Z. marina*. We quantified the variable oxygen environment in the rhizomes of *Phyllospadix spp.* to determine if they allow for aerobic as well as anaerobic metabolisms. We analyzed the microbial taxa present and examined their gene content to estimate their functional and metabolic capacities. We hypothesized that microbial partners: 1) enhance host access to dissolved inorganic nitrogen through nitrogen recycling, ammonification and nitrogen fixation, 2) provision vitamins B_1, B_2, B_7, B_{12}, and 3) use a diversity of abundant dissolved organic carbon exudates from the host. We tested whether microbial taxonomy and function differed across hosts and host tissue types, and whether anaerobic metabolisms were present in low-O_2 environments (e.g., rhizomes and sediment). Through this study, we find that the range of oxygen environments engineered by host phototrophs likely explains the diversity of both oxidizing and reducing microbial metabolisms, and contributes to the functional capabilities of microbes and their influence on carbon and nitrogen cycling in nearshore ecosystems.

Methods

Sampling and DNA Extraction

We collected metagenome samples from the surfaces of 5 different phototroph species (Table S1). The surface of *Phyllospadix scouleri* blades, *Laminaria setchellii* fronds and the inner bulbs of *Nereocystis luetkeana* were swabbed with a sterile swab and brushed with an interdental brush (GUM Proxabrush Go-Betweens). We preserved sections of the rhizomes of *Phyllospadix scouleri*, *P. serrulatus* and *Zostera marina*. Sediment surrounding *P. scouleri* and *Z. marina* was also collected. All samples were collected from Tatoosh Island, WA, USA (48.393679, -124.734617) on 16-17 Jul 2019, except for *Z. marina* samples which were sampled from West

bioRxiv preprint doi: https://doi.org/10.1101/2022.01.05.475171; this version posted January 7, 2022. The copyright holder for this preprint (which was not certified by peer review) is the author/funder, who has granted bioRxiv a license to display the preprint in perpetuity. It is made available under aCC-BY-ND 4.0 International license.

Falmouth Bay, MA, USA (41.60708333, -70.64527778) on 19 Sept 2019. We included samples from the rhizosphere of *Z. marina* from the Atlantic Ocean as a known positive control for nitrogen fixation (22, 23). Swabs, tissue and sediment were immediately frozen at 20° C and shipped to storage at -80° C. DNA from these collections was extracted with a Qiagen PowerSoil Kit and multiple samples were pooled for each metagenome sample to increase DNA quantity and possible discovery: *P. scouleri* blade, rhizome and sediment (3 pooled individuals each), *P. serrulatus* rhizome (3 individuals), *L. setchellii blade* (3 individuals), *N. luetkeana* interior bulb (4 individuals), *Z. Marina* rhizomes and sediment (2 individuals).

Shotgun metagenomic sequencing, assembly, and read recruitment

The above 8 samples were run over 2 lanes on a HiSeq 2500 (2x150) with TruSeq DNA library preps at Argonne National Laboratory. For each sample, resulting DNA sequences were first quality filtered (35)(Minoche et al. 2011), then assembled with IDBA-UD v1.1.3 (36) (Peng et al. 2012) with a minimum scaffold length of 1 kbp. Metagenomic short reads from each sample were then recruited back to their corresponding assembled contigs using Bowtie2 (37). Samtools (38) was used to generate sorted and indexed BAM files. Anvi'o v7.0 (39) was used as the command line environment for all downstream analyses. 'anvi-gen-contigs-database' was used to generate anvi'o contigs databases, during which Prodigal v2.6.3 (40) identified open reading frames, and 'anvi-run-hmms' was used to identify genes matching to archaeal and bacterial single-copy core gene collections using HMMER (41).

Reconstructing metagenome-assembled genomes (MAGs)

bioRxiv preprint doi: https://doi.org/10.1101/2022.01.05.475171; this version posted January 7, 2022. The copyright holder for this preprint (which was not certified by peer review) is the author/funder, who has granted bioRxiv a license to display the preprint in perpetuity. It is made available under aCC-BY-ND 4.0 International license.

To reconstruct genomes from the assembled metagenomes, we used a combination of automatic binning via CONCOCT v1.1.0 (42), followed by a manual curation of each MAG as outlined by Shaiber et al. 2020 (43). Genome taxonomy was determined using GTDB v.1.3.0 (44), and 'anvi-run-scg-taxonomy'. We also inferred gene-level taxonomy using Centrifuge v1.0.4 (45) to aid manual curation.

Phylogenomic analysis of MAGs

To perform a phylogenomic analysis of our MAGs, we recovered amino acid sequences for bacterial single-copy core genes (SCGs) from each genome (except the only archaeal genome in our collection) using the program ‘anvi-get-sequences-for-hmm-hits’ with the parameter `--hmm-source `Bacteria_71` on the ribosomal gene set `Ribosomal L1-L6` and the flag `--concatenate`, which independently aligned each SCG independently using Muscle v3.8.1 (46) before concatenating them into a final superalignment. We then refined the alignment using trimAl v1.4.rev15 (47) to remove any position in the alignment if more than 50% of the residues were gap characters. A maximum-likelihood phylogeny was inferred using IQTree (48) with 1,000 bootstrap replicates, and a LG+R6 model best fit our data using ModelFinder (49).

Functional analysis of microbial communities

To address the metabolic capabilities of host-associated microbes, we annotated genes in each anvi’o contigs database with 3 different databases using ‘anvi-run-kegg-kofams’, ‘anvi-run-ncbi-cogs’, and ‘anvi-run-pfams’, which used the databases of Kyoto Encyclopedia of Genes and Genomes (KEGG) (50), NCBI’s Clusters of Orthologous Genes (COGs) (51) and EBI’s Pfam database (52) respectively. We used these annotated genes to test for 1) nitrogen cycling

bioRxiv preprint doi: https://doi.org/10.1101/2022.01.05.475171; this version posted January 7, 2022. The copyright holder for this preprint (which was not certified by peer review) is the author/funder, who has granted bioRxiv a license to display the preprint in perpetuity. It is made available under aCC-BY-ND 4.0 International license.

183 metabolisms, especially those within the nitrogen-fixation pathway, 2) hydrolases, including
184 ureases, as well as ammonia-lyases, to cleave the C-N bonds in amino acids and make
185 ammonium available to the host, 3) vitamin production, namely vitamins B_1, B_2, B_7 and B_{12} and
186 4) a set of dissolved organic matter (DOM) transporter genes identified by Poretsky et al. (34)
187 that indicate the ability of the microbial community to assimilate DOM exudates from kelps and
188 surfgrasses. The list of genes used is indicated in Table S4. We additionally developed and used
189 a graph-based algorithm on KEGG definitions for vitamins B_1, B_2, B_7 and B_{12} to detect the
190 presence of these biosynthetic pathways (Supplementary Code 1). To expand our functional
191 analysis of kelp blade genes, we included 32 MAGs from the surface of *N. luetkeana* blades that
192 were collected from the same location at the same time using similar methods as those described
193 above (53).
194
195 *Phylogenetic analysis of nifH genes*
196 To search for *nifH* amino acid sequences in our environmental samples, we identified 9 MAGs
197 which contained *nifH* genes using the KEGG identifier K02588 with e-value < 1e-20. We
198 aligned the AA sequences for these genes against 89 well-characterized reference *nifH* AA
199 sequences (Table S6) using Muscle v3.8.1 (46) and refined the alignment using trimAl (gap-
200 threshold: 0.5) and 'anvi-script-reformat-fasta' (max-percentage-gap: 50%). A maximum-
201 likelihood phylogeny was inferred using IQTree (48) with 1,000 bootstrap replicates, and a
202 LG+R5 model best fit our data using ModelFinder (49). *nifH* genes from the *Zostera* samples
203 served as positive controls to detect nitrogen fixation genes in other samples. Figures 2, 3, 4 were
204 generated using iTol v5 (54), R v4.0.3 and FigTree respectively. We additionally took tissue
205 samples from *P. scouleri* rhizome (n = 16), basal meristematic region just distal to the sheath

bioRxiv preprint doi: https://doi.org/10.1101/2022.01.05.475171; this version posted January 7, 2022. The copyright holder for this preprint (which was not certified by peer review) is the author/funder, who has granted bioRxiv a license to display the preprint in perpetuity. It is made available under aCC-BY-ND 4.0 International license.

(n = 12) and blade 35 cm above the rhizome (n = 12) to quantify stable isotopes of δ15N and δ13C to look for signatures of nitrogen fixation (methods described in Appendix 1).

Quantifying the Oxygen Environment

We quantified the oxygen concentrations in proximity to *Phyllospadix spp.* rhizomes by comparing dissolved oxygen (DO) concentrations in the surrounding seawater and in the sediment around the rhizome. We used a Pyro Science Robust Oxygen Probe (OXROB10, Firesting™, Pyroscience), and repeated measurements around 0900h across 4 days (7-9 June 2019, 13 June 2021) within *P. scouleri* (n = 18) and *P. serrulatus* (n = 11) rhizomes. Each reading first measured the surrounding seawater after which we gently pushed the tip of the oxygen probe into the sediment and rhizome mass to a depth of 1-3 mm, the typical thickness (*pers. observation*). We let the probe equilibrate and took a reading at 150 sec. This allowed the rhizome oxygen environment to equilibrate after we disturbed the intact rhizome. We compared surrounding water and within-rhizome oxygen using paired t-tests in R.

Data Availability

In addition to the code available on GitHub (___), the final MAG database files generated in anvi'o are available on the FigShare repository: (_____). Metagenomic sequence data are available at the NCBI's Sequence Read Archive under accession no. (submission in progress).

Results

Surfgrass rhizomes have lower oxygen concentrations than surrounding seawater

bioRxiv preprint doi: https://doi.org/10.1101/2022.01.05.475171; this version posted January 7, 2022. The copyright holder for this preprint (which was not certified by peer review) is the author/funder, who has granted bioRxiv a license to display the preprint in perpetuity. It is made available under aCC-BY-ND 4.0 International license.

The oxygen environment in the rhizomes differed significantly from that of the surrounding seawater (Fig. 1). Rhizomes maintained a lower dissolved oxygen (DO) concentration than the surrounding seawater for both *P. scouleri* (n=18, pairwise t-test: $p<0.001$) and *P. serrulatus* (n=11, pairwise t-test: $p<0.001$). *P. serrulatus* maintained a slightly lower DO concentration in the rhizome at 2.11 mg l^{-1}, compared to 5.61 mg l^{-1} for *P. scouleri*. However, the nature of sampling likely introduced more oxygenated water from the surrounding water column to the rhizome-sediment microenvironment, suggesting that the actual DO concentration within the sediment is lower than the value reported.

Diversity of MAGs assembled across hosts

Following filtering, we obtained an average of 41 million reads per sample (range 6.48 to 67.73 million), with 79.8% of raw reads retained on average. When these reads were assembled into contigs of at least 1000 nucleotides, a mean of 42,026 contigs and a mean of 110,054 genes were present across samples (Table S1).

Across 8 metagenomes we manually binned 33 high quality MAGs, defined as having a completion score >90% and contamination (or redundancy) < 10% (Table 2). We also identified 39 lower quality MAGs that had completion scores between 38 and 93% and redundancy scores between 0 and 21% (Table S3). All MAGs were bacterial except for a single archaeal MAG on the rhizome of *P. scouleri*. The bacterial MAGs spanned 7 phyla, including *Proteobacteria* (n=34), *Bacteroidota* (n=19), *Verrumicrobia* (n=2), *Campylobacterota* (n=3), *Desulfobacterota* (n=5), and a single MAG in each of *Desulfomonadota*, *Acidobacteriota*, and *Spirochaetota*. The Archaea belonged to the phylum *Chrenarchaeota*. There were 46 MAGs resolved to the species

bioRxiv preprint doi: https://doi.org/10.1101/2022.01.05.475171; this version posted January 7, 2022. The copyright holder for this preprint (which was not certified by peer review) is the author/funder, who has granted bioRxiv a license to display the preprint in perpetuity. It is made available under aCC-BY-ND 4.0 International license.

level, with 8 to the genus level, 9 to family, 2 to order, and 2 to class level. Five MAGs were resolved only as Bacteria (Table S2).

The 72 MAGs belong to diverse microbial phyla, which were distributed across the 5 host species and tissue types (Fig. 2). In some cases, bacterial taxa from kelp blade tissues were most closely related to bacteria collected from the rhizome or sediment of a seagrass, suggesting that closely related bacterial taxa can associate with diverse hosts. Known anaerobic sulfur cyclers like *Desulfobulbia, Desulfobacteria, Desulfuromonadia* and *Campylobacteria* (*Sulfurovum sp000296775* and *Sulfurimonas autotrophica*) were exclusively found in the low oxygen rhizome and sediment samples of *Zostera marina* and *Phyllospadix spp*. Conversely, *Alphaproteobacteria*, were exclusively found on surfaces exposed to the water column. *Gammaproteobacteria* was the only class found across the range of tissue types (6 out of 8 host environments). We did not include the only well-resolved archaeal taxon found in our samples, *Crenarchaea* (*P. scouleri* rhizome), as our analysis compared single-copy core genes specific to bacterial phyla.

Host-associated microbial genomes contain pathways to synthesize vitamins, recycle nitrogen, and use host-generated carbon

We found evidence for a number of metabolic pathways that are likely important for exchanges between host phototrophs and their microbial partners (Fig. 3). Microbes on hosts had genes for diverse carbohydrate and carboxylic acid assimilation via cell membrane transport proteins. Host-associated microbes also had genes for a diversity of nitrogen metabolisms, including ureases and hydrolases that could regenerate ammonium. Nitrogen metabolisms were most

bioRxiv preprint doi: https://doi.org/10.1101/2022.01.05.475171; this version posted January 7, 2022. The copyright holder for this preprint (which was not certified by peer review) is the author/funder, who has granted bioRxiv a license to display the preprint in perpetuity. It is made available under aCC-BY-ND 4.0 International license.

diverse in rhizome and sediment samples where we identified both oxidizing (nitrification) and reducing (nitrate reduction, nitrogen fixation, denitrification) metabolisms, as well as metabolisms that both oxidize and reduce (annamox).

Every sample had at least one gene from B-vitamins biosynthesis pathways. Using a simple-path based algorithm on KEGG definitions (Supplementary Code 1), we determined that all microbial communities had the metabolic pathways to synthesize vitamins B_1 (with the exception of the *P. scouleri* rhizome), B_2 and B_7 (except inside the bulb of *N. luetkeana*). The Vitamin B_{12} anaerobic biosynthesis pathway, however, was only present in MAGs found on the blades of *L. setchellii* (2) and *P. scouleri* (3) and the rhizomes of *P. serrulatus* (2) and *Z. marina* (1). Additionally, all three MAGs on the blade of *P. scouleri* that had this anaerobic pathway had the genes necessary to synthesize Vitamin B_{12} aerobically as well.

Novel detection of nifH *genes in surfgrass*

We identified the nitrogenase gene (*nifH*) in 9 MAGs with e-value support < 1.3e-120 (KEGG) and < 1.1e-135 (COG). These 9 MAGs were assembled from *P. serrulatus* rhizomes (n = 2) and *Z. marina* rhizomes (n = 3) and the surrounding sediment (n = 4). Of these 9 MAGs, 5 were resolved to the genus level, while others were resolved to the order and family level, including *Campylobacterales*, *Desulfobacterales* and 2 *Flavobacteriaceae* (Fig. 4, Table S5). *nifH* genes identified in the rhizomes of *P. serrulatus* and *Z. marina* belonging to the class *Desulfobacteria* and family *Flavobacteriaceae*, clustered within Cluster III: anaerobic nitrogen-fixers that are often coupled with sulfate-reduction metabolisms. Samples from *Z. marina* sediment and rhizome also contained 3 *nifH* genes in *Campylobacterial* MAGs that clustered together in a

bioRxiv preprint doi: https://doi.org/10.1101/2022.01.05.475171; this version posted January 7, 2022. The copyright holder for this preprint (which was not certified by peer review) is the author/funder, who has granted bioRxiv a license to display the preprint in perpetuity. It is made available under aCC-BY-ND 4.0 International license.

297 sister clade to the aerobic nitrogen-fixers of Cluster I. The COG gene identified as *nifH*
298 (COG1348) also includes the homologous protochlorophyllides, which are involved in
299 photosynthetic pigment synthesis but have high sequence similarity to the *nifH* gene (21, 55).
300 Instead, we used the KEGG gene (K02588) that does not detect these homologs. When we
301 inspected genes on the same contig with *nifH*, we found a number of genes related to nitrogen
302 fixation (Table S5), including *nifD* (COG 2710) in 7 of the 9 contigs, nitrogen regulatory protein
303 PII (COG 347), *nifB* (COG 535), and multiple iron containing proteins including ferrodoxin and
304 Fe-Mo cluster-binding proteins (Table S5).
305

306 **Discussion**

307 *Phototroph tissues and sediment host distinct microbial taxa and functions*
308 The phototroph species we sampled in this study are foundational in coastal ecosystems (56–59),
309 yet a description of the diversity and function of their microbiomes have been lacking. All
310 MAGs were bacterial, except for a single archaeal MAG (*Crenarchaeota*) in the rhizome of
311 *Phyllospadix scouleri*, which was identified as *Nitrosopumulis*, a genus associated with
312 nitrification (Table S3). Together, these 5 phototrophs hosted bacteria from 9 phyla. The only
313 low diversity sample was the interior of the bulb of *Nereocystis*, where we assembled only a
314 single MAG (*UBA7415 sp002470515*) suggesting that this environment of high carbon
315 monoxide and nitrogen gas (60) may inhibit microbial activity or pose a highly selective
316 environment. Blades of kelp and surfgrass, in contrast, were a locus of microbial diversity and
317 function, a finding that is similar to many recent studies of macroalgal and seagrass microbiomes
318 reporting high microbial diversity (2, 4, 5, 61–63). The functional attributes of microbial taxa
319 associated with marine macrophytes include pathogen resistance (64), the ability to provision the

bioRxiv preprint doi: https://doi.org/10.1101/2022.01.05.475171; this version posted January 7, 2022. The copyright holder for this preprint (which was not certified by peer review) is the author/funder, who has granted bioRxiv a license to display the preprint in perpetuity. It is made available under aCC-BY-ND 4.0 International license.

host with B vitamins (9), and enhanced host algal fitness (65), perhaps through some of the nitrogen metabolisms we documented here (14, 66).

Host-microbe interactions in a dynamic oxygen microenvironment

Grouping MAGs by microbial metabolisms (Fig. 3) showed key functional differences among phototroph hosts. Blade tissues that interacted directly with the water column were associated with microbial nitrogen metabolisms that were mostly oxidizing. The abundance of dissolved organic carbon from phototroph hosts (29–31, 59) might select for heterotrophic metabolisms. Indeed, we found an abundance of genes for dissolved organic matter assimilation and transport in all metagenomes, suggesting that hosts may stimulate heterotrophy in their associated microbial community similar to findings by Poretsky et al. (34). Improved characterization of the components of dissolved organic matter and the genomes of hosts will allow us to better assess complementarity in resource supply by hosts and resource use by microbes.

The host tissue types in this study differed in surface oxygen concentrations. Blade tissue interacts with the water column and is likely more oxygenated than rhizome tissue or sediments, though a previous study suggests there can also be a 60% reduction in oxygen along the immediate surface of kelp blades (67), and along the mucus layer where some kelp-associated bacteria reside (6). Over two-thirds of the bacterial taxa on blades of *N. luetkeana* belonged to families associated with obligately aerobic metabolisms, demonstrating the role of oxygen in shaping phototroph-associated microbial communities (68). The sediment surrounding the rhizomes of *Phyllospadix spp.* contained low oxygen microenvironments (Fig. 1) likely maintained by macroinvertebrate respiration (69)(Moulton and Hacker 2011), similar to the

bioRxiv preprint doi: https://doi.org/10.1101/2022.01.05.475171; this version posted January 7, 2022. The copyright holder for this preprint (which was not certified by peer review) is the author/funder, who has granted bioRxiv a license to display the preprint in perpetuity. It is made available under aCC-BY-ND 4.0 International license.

343 biological processes in the anaerobic sediment surrounding *Zostera* (13). Low rhizosphere
344 oxygen concentrations likely structured the taxonomic composition of *Z. marina* to include
345 anaerobic taxa such as *Campylobacteria*, *Desulfatitalea* and *Desulfobulbus*. The presence of
346 anaerobes like *Desulfuromonadia*, *Desulfobaceria*, *Spirochaeta* and *Aminicenantia* in *P.*
347 *serrulatus* rhizomes suggests sulfate reduction also occurs, possibly coupled to dissolved organic
348 carbon use as an energy source (e.g. (70) Howarth & Hobbie 1982). Additionally,
349 *Campylobacteria* and the genus *Thiodiazotropha* were associated with *Z. marina* and may
350 remove detrimental sulfide accumulation through sulfur oxidation (71, 72).
351
352 Nitrogen metabolisms that were both oxidizing and reducing were found in MAGs associated
353 with rhizomes of both *Z. marina* and *Phyllospadix* (Fig. 3), suggesting the potential for temporal
354 niches when, for example, ammonium oxidation to nitrate occurs during high-O_2 daylight
355 periods, followed by nitrate reduction or nitrogen fixation during O_2-depleted nighttime hours.
356 Additionally, all MAGs in this study contained hydrolases that cleave carbon-nitrogen bonds to
357 produce ammonium (14), recycling nitrogen compounds for host uptake. Oxidizing and reducing
358 metabolisms are likely separated only by microns in the hosts studied here.
359
360 We detected biosynthetic pathways for vitamins B_1, B_2, B_7 and B_{12} that are required by the
361 auxotrophic phototroph hosts in this study (9, 10, 73). We found that only the blades of *P.*
362 *scouleri* harbored MAGs with both anaerobic and aerobic biosynthetic pathways for Vitamin
363 B_{12}, suggesting that the variable oxygen environment driven by host-metabolism creates diverse
364 metabolic niches for associated microbes. Strong gradients in oxygen and metabolically diverse
365 microbial metabolisms are present in a diversity of animal hosts such as corals and sponges as a

bioRxiv preprint doi: https://doi.org/10.1101/2022.01.05.475171; this version posted January 7, 2022. The copyright holder for this preprint (which was not certified by peer review) is the author/funder, who has granted bioRxiv a license to display the preprint in perpetuity. It is made available under aCC-BY-ND 4.0 International license.

result of host metabolism (74–76). Fluctuating oxygen microenvironments might also promote cross-feeding, where microbial taxa produce a metabolite that can be consumed by other taxa. Cross-feeding is potentially important for nitrogen (77) and carbon metabolisms (78, 79) in microbial communities.

Characteristics of previously undescribed nitrogen fixation in surfgrass

Building on recent studies that illustrate the association of nitrogen fixing microbes with a diversity of macroalgae (80) and seagrasses (22, 23, 81, 82), we found a previously undescribed diversity of nitrogenase genes associated with the surfgrass *Phyllospadix*. We detected *nifH* genes in *P. serrulatus* rhizomes that resolved into the Cluster I group of nifH genes, which are characterized by aerobic nitrogen fixers. *P. serrulatus*, in comparison to *P. scouleri*, is found higher up in the intertidal zone and often in sheltered tidepools that tend to undergo dramatic daily fluctuations in oxygen, possibly allowing for a temporal low-O_2 niche during the night (83). Conversely, we did not detect nitrogenase genes in the microbiome of *P. scouleri*, which inhabits more wave-exposed and thus better oxygenated environments (Fig. 1). However, stable isotope analyses across *P. scouleri* samples show a lower nitrogen isotopic signature in the rhizome compared to the rest of the plant, a possible indication of nitrogen from an atmospheric source (Fig. S1), though *in situ* experiments with stable isotope tracers are needed to confirm the presence of nitrogen fixation.

Nitrogen fixation by microbial associates provides a key means of increasing the availability of ammonium, possibly supporting primary productivity. *P. scouleri* biomass reaches 12.7 kg of wet mass per square meter of shore and exudes 0.93 mg C per hour per gram dry mass as

bioRxiv preprint doi: https://doi.org/10.1101/2022.01.05.475171; this version posted January 7, 2022. The copyright holder for this preprint (which was not certified by peer review) is the author/funder, who has granted bioRxiv a license to display the preprint in perpetuity. It is made available under aCC-BY-ND 4.0 International license.

389 dissolved organic carbon that may fuel microbial activity (59). There is evidence that nitrogen
390 fixation can contribute to seagrass productivity (66, 84), a possible adaptation to low nitrogen
391 environments. Our finding that nitrogen fixing microbes are associated with a rocky intertidal
392 surfgrass is especially surprising given that Tatoosh Island is in an area of upwelling and high
393 DIN (86) at the more northerly end of the California Current Large Marine Ecosystem. Whether
394 nitrogen fixation forms the basis for reciprocal host-microbe exchange is still unknown.
395
396 The metagenomic analyses we present here suggest that phototroph-associated microbiomes may
397 be involved in carbon, nitrogen and vitamin metabolisms important to their hosts, likely
398 generating commensal or mutualistic interactions. Future experiments should test these
399 hypothesized interactions between host and microbiome. The importance of seaweeds and
400 seagrasses to coastal productivity, and the demonstrated sensitivity of both host and microbes to
401 increasing temperatures and pH (11, 62, 85), pathogens (61), and other anthropogenic stressors,
402 underline the importance of further studying phototroph-microbiome interactions.
403
404 **Acknowledgements**

405 Our gratitude to the Makah Tribal Nation for access to Tatoosh Island. We thank The University
406 of Chicago's Microbiome Center for pilot award funding, and Washington Department of
407 Natural Resources grants 93099282, 93100399 (CAP) and NSF-DEB grant (#1556874) awarded
408 to JT Wootton. We appreciate the work of C Sauceda in the isotope analysis, and A Wootton, A
409 Wood and K Foreman in the field sampling. KM was supported by an EE Fellowship from The
410 University of Chicago. S Owens and S Greenwald at Argonne National Lab provided expertise
411 in sequencing.

bioRxiv preprint doi: https://doi.org/10.1101/2022.01.05.475171; this version posted January 7, 2022. The copyright holder for this preprint (which was not certified by peer review) is the author/funder, who has granted bioRxiv a license to display the preprint in perpetuity. It is made available under aCC-BY-ND 4.0 International license.

412 **References**

413 1. McFall-Ngai M, Hadfield MG, Bosch TCG, Carey HV, Domazet-Lošo T, Douglas AE,
414 Dubilier N, Eberl G, Fukami T, Gilbert SF, Hentschel U, King N, Kjelleberg S, Knoll AH,
415 Kremer N, Mazmanian SK, Metcalf JL, Nealson K, Pierce NE, Rawls JF, Reid A, Ruby EG,
416 Rumpho M, Sanders JG, Tautz D, Wernegreen JJ. 2013. Animals in a bacterial world, a new
417 imperative for the life sciences. Proc Natl Acad Sci USA 110:3229–3236.
418 2. Weigel BL, Pfister CA. 2019. Successional Dynamics and Seascape-Level Patterns of
419 Microbial Communities on the Canopy-Forming Kelps Nereocystis luetkeana and Macrocystis
420 pyrifera. Frontiers in Microbiology 10:346.
421 3. Lemay MA, Martone PT, Keeling PJ, Burt JM, Krumhansl KA, Sanders RD, Wegener
422 Parfrey L. 2018. Sympatric kelp species share a large portion of their surface bacterial
423 communities: Kelp-associated bacterial diversity. Environmental Microbiology 20:658–670.
424 4. Quigley CTC, Capistrant-Fossa KA, Morrison HG, Johnson LE, Morozov A, Hertzberg
425 VS, Brawley SH. 2020. Bacterial Communities Show Algal Host (Fucus spp.)/Zone
426 Differentiation Across the Stress Gradient of the Intertidal Zone. Front Microbiol 11:563118.
427 5. Lemay MA, Davis KM, Martone PT, Parfrey LW. 2021. Kelp-associated Microbiota are
428 Structured by Host Anatomy [1]. J Phycol 57:1119–1130.
429 6. Ramirez-Puebla ST, Weigel BL, Jack L, Schlundt C, Pfister CA, Mark Welch JL. 2020.
430 Spatial organization of the kelp microbiome at micron scales. preprint, Microbiology.
431 7. Jacoby R, Peukert M, Succurro A, Koprivova A, Kopriva S. 2017. The Role of Soil
432 Microorganisms in Plant Mineral Nutrition—Current Knowledge and Future Directions. Front
433 Plant Sci 8:1617.
434 8. Mills MM, Turk-Kubo KA, van Dijken GL, Henke BA, Harding K, Wilson ST, Arrigo

bioRxiv preprint doi: https://doi.org/10.1101/2022.01.05.475171; this version posted January 7, 2022. The copyright holder for this preprint (which was not certified by peer review) is the author/funder, who has granted bioRxiv a license to display the preprint in perpetuity. It is made available under aCC-BY-ND 4.0 International license.

435 KR, Zehr JP. 2020. Unusual marine cyanobacteria/haptophyte symbiosis relies on N2 fixation
436 even in N-rich environments. The ISME Journal https://doi.org/10.1038/s41396-020-0691-6.
437 9. Croft MT, Lawrence AD, Raux-Deery E, Warren MJ, Smith AG. 2005. Algae acquire
438 vitamin B12 through a symbiotic relationship with bacteria. Nature 438:90–93.
439 10. Wichard T, Charrier B, Mineur F, Bothwell JH, Clerck OD, Coates JC. 2015. The green
440 seaweed Ulva: a model system to study morphogenesis. Front Plant Sci 6.
441 11. Qiu Z, Coleman MA, Provost E, Campbell AH, Kelaher BP, Dalton SJ, Thomas T,
442 Steinberg PD, Marzinelli EM. 2019. Future climate change is predicted to affect the microbiome
443 and condition of habitat-forming kelp. Proceedings of the Royal Society B: Biological Sciences
444 286:20181887.
445 12. Bell W, Mitchell R. 1972. Chemotactic and Growth Responses of Marine Bacteria to
446 Algal Extracellular Products. Biological Bulletin 143:265–277.
447 13. Brodersen KE, Siboni N, Nielsen DA, Pernice M, Ralph PJ, Seymour J, Kühl M. 2018.
448 Seagrass rhizosphere microenvironment alters plant-associated microbial community
449 composition. Environ Microbiol 20:2854–2864.
450 14. Tarquinio F, Bourgoure J, Koenders A, Laverock B, Säwström C, Hyndes GA. 2018.
451 Microorganisms facilitate uptake of dissolved organic nitrogen by seagrass leaves. The ISME
452 Journal https://doi.org/10.1038/s41396-018-0218-6.
453 15. Ladd JN, Jackson RB. 1982. Biochemistry of Ammonification, p. 173–228. *In* Stevenson,
454 FJ (ed.), Agronomy Monographs. American Society of Agronomy, Crop Science Society of
455 America, Soil Science Society of America, Madison, WI, USA.
456 16. Delmont TO, Quince C, Shaiber A, Esen ÖC, Lee ST, Rappé MS, McLellan SL, Lücker
457 S, Eren AM. 2018. Nitrogen-fixing populations of Planctomycetes and Proteobacteria are

bioRxiv preprint doi: https://doi.org/10.1101/2022.01.05.475171; this version posted January 7, 2022. The copyright holder for this preprint (which was not certified by peer review) is the author/funder, who has granted bioRxiv a license to display the preprint in perpetuity. It is made available under aCC-BY-ND 4.0 International license.

458 abundant in surface ocean metagenomes. Nature Microbiology 3:804–813.

459 17. Sohm JA, Webb EA, Capone DG. 2011. Emerging patterns of marine nitrogen fixation.

460 Nat Rev Microbiol 9:499–508.

461 18. Bombar D, Paerl RW, Riemann L. 2016. Marine Non-Cyanobacterial Diazotrophs:

462 Moving beyond Molecular Detection. Trends in Microbiology 24:916–927.

463 19. Harding K, Turk-Kubo KA, Sipler RE, Mills MM, Bronk DA, Zehr JP. 2018. Symbiotic

464 unicellular cyanobacteria fix nitrogen in the Arctic Ocean. Proc Natl Acad Sci USA 115:13371–

465 13375.

466 20. Cabello AM, Turk-Kubo KA, Hayashi K, Jacobs L, Kudela RM, Zehr JP. 2020.

467 Unexpected presence of the nitrogen-fixing symbiotic cyanobacterium UCYN-A in Monterey

468 Bay, California. J Phycol 56:1521–1533.

469 21. Raymond J, Siefert JL, Staples CR, Blankenship RE. 2004. The Natural History of

470 Nitrogen Fixation. Molecular Biology and Evolution 21:541–554.

471 22. Patriquin D, Knowles R. 1972. Nitrogen fixation in the rhizosphere of marine

472 angiosperms. Marine Biology 16:49–58.

473 23. Capone DG. 1982. Nitrogen Fixation (Acetylene Reduction) by Rhizosphere Sediments

474 of the Eelgrass Zostera marina. Marine Ecology Progress Series 10:67–75.

475 24. Cole L, McGlathery K. 2012. Nitrogen fixation in restored eelgrass meadows. Marine

476 Ecology Progress Series 448:235–246.

477 25. Agawin N, Ferriol P, Sintes E. 2019. Simultaneous measurements of nitrogen fixation in

478 different plant tissues of the seagrass Posidonia oceanica. Mar Ecol Prog Ser 611:111–127.

479 26. Aoki L, McGlathery K. 2019. High rates of N fixation in seagrass sediments measured

480 via a direct 30N2 push-pull method. Mar Ecol Prog Ser 616:1–11.

bioRxiv preprint doi: https://doi.org/10.1101/2022.01.05.475171; this version posted January 7, 2022. The copyright holder for this preprint (which was not certified by peer review) is the author/funder, who has granted bioRxiv a license to display the preprint in perpetuity. It is made available under aCC-BY-ND 4.0 International license.

481 27. Massey V. 2000. The chemical and biological versatility of riboflavin. 28:283–296.

482 28. Grossman A. 2016. Nutrient Acquisition: The Generation of Bioactive Vitamin B 12 by

483 Microalgae. Current Biology 26:R319–R321.

484 29. Reed DC, Carlson CA, Halewood ER, Nelson JC, Harrer SL, Rassweiler A, Miller RJ.

485 2015. Patterns and controls of reef-scale production of dissolved organic carbon by giant kelp *M*

486 *acrocystis pyrifera*: DOC production by giant kelp. Limnology and Oceanography 60:1996–

487 2008.

488 30. Weigel BL, Pfister CA. 2021. The dynamics and stoichiometry of dissolved organic

489 carbon release by kelp. Ecology 102.

490 31. Wetzel RG, Penhale PA. 1979. Transport of carbon and excretion of dissolved organic

491 carbon by leaves and roots/rhizomes in seagrasses and their epiphytes. Aquatic Botany 6:149–

492 158.

493 32. Barrón C, Apostolaki ET, Duarte CM. 2014. Dissolved organic carbon fluxes by seagrass

494 meadows and macroalgal beds. Frontiers in Marine Science 1.

495 33. Pfister CA, Altabet MA. 2019. Enhanced microbial nitrogen transformations in

496 association with macrobiota from the rocky intertidal. Biogeosciences 16:193–206.

497 34. Poretsky RS, Sun S, Mou X, Moran MA. 2010. Transporter genes expressed by coastal

498 bacterioplankton in response to dissolved organic carbon. Environmental Microbiology 12:616–

499 627.

500 35. Minoche AE, Dohm JC, Himmelbauer H. 2011. Evaluation of genomic high-throughput

501 sequencing data generated on Illumina HiSeq and Genome Analyzer systems. Genome Biol

502 12:R112.

503 36. Peng Y, Leung HCM, Yiu SM, Chin FYL. 2012. IDBA-UD: a de novo assembler for

bioRxiv preprint doi: https://doi.org/10.1101/2022.01.05.475171; this version posted January 7, 2022. The copyright holder for this preprint (which was not certified by peer review) is the author/funder, who has granted bioRxiv a license to display the preprint in perpetuity. It is made available under aCC-BY-ND 4.0 International license.

504 single-cell and metagenomic sequencing data with highly uneven depth. Bioinformatics
505 28:1420–1428.
506 37. Langmead B, Salzberg SL. 2012. Fast gapped-read alignment with Bowtie 2. Nat
507 Methods 9:357–359.
508 38. Li H, Handsaker B, Wysoker A, Fennell T, Ruan J, Homer N, Marth G, Abecasis G,
509 Durbin R, 1000 Genome Project Data Processing Subgroup. 2009. The sequence alignment/map
510 format and SAMtools. Bioinformatics 25:2078–2079.
511 39. Eren AM, Kiefl E, Shaiber A, Veseli I, Miller SE, Schechter MS, Fink I, Pan JN, Yousef
512 M, Fogarty EC, Trigodet F, Watson AR, Esen ÖC, Moore RM, Clayssen Q, Lee MD, Kivenson
513 V, Graham ED, Merrill BD, Karkman A, Blankenberg D, Eppley JM, Sjödin A, Scott JJ,
514 Vázquez-Campos X, McKay LJ, McDaniel EA, Stevens SLR, Anderson RE, Fuessel J,
515 Fernandez-Guerra A, Maignien L, Delmont TO, Willis AD. 2021. Community-led, integrated,
516 reproducible multi-omics with anvi'o. Nat Microbiol 6:3–6.
517 40. Hyatt D, Chen G-L, LoCascio PF, Land ML, Larimer FW, Hauser LJ. 2010. Prodigal:
518 prokaryotic gene recognition and translation initiation site identification. BMC Bioinformatics
519 11:119.
520 41. Eddy SR. 2011. Accelerated Profile HMM Searches. PLoS Comput Biol 7:e1002195.
521 42. Alneberg J, Bjarnason BS, de Bruijn I, Schirmer M, Quick J, Ijaz UZ, Lahti L, Loman
522 NJ, Andersson AF, Quince C. 2014. Binning metagenomic contigs by coverage and composition.
523 Nat Methods 11:1144–1146.
524 43. Shaiber A, Willis AD, Delmont TO, Roux S, Chen L-X, Schmid AC, Yousef M, Watson
525 AR, Lolans K, Esen ÖC, Lee STM, Downey N, Morrison HG, Dewhirst FE, Mark Welch JL,
526 Eren AM. 2020. Functional and genetic markers of niche partitioning among enigmatic members

bioRxiv preprint doi: https://doi.org/10.1101/2022.01.05.475171; this version posted January 7, 2022. The copyright holder for this preprint (which was not certified by peer review) is the author/funder, who has granted bioRxiv a license to display the preprint in perpetuity. It is made available under aCC-BY-ND 4.0 International license.

527 of the human oral microbiome. Genome Biol 21:292.

528 44. Parks DH, Chuvochina M, Rinke C, Mussig AJ, Chaumeil P-A, Hugenholtz P. 2021.

529 GTDB: an ongoing census of bacterial and archaeal diversity through a phylogenetically

530 consistent, rank normalized and complete genome-based taxonomy. Nucleic Acids Research

531 gkab776.

532 45. Kim D, Song L, Breitwieser FP, Salzberg SL. 2016. Centrifuge: rapid and sensitive

533 classification of metagenomic sequences. Genome Res 26:1721–1729.

534 46. Edgar RC. 2004. MUSCLE: multiple sequence alignment with high accuracy and high

535 throughput. Nucleic Acids Research 32:1792–1797.

536 47. Capella-Gutierrez S, Silla-Martinez JM, Gabaldon T. 2009. trimAl: a tool for automated

537 alignment trimming in large-scale phylogenetic analyses. Bioinformatics 25:1972–1973.

538 48. Nguyen L-T, Schmidt HA, von Haeseler A, Minh BQ. 2015. IQ-TREE: A Fast and

539 Effective Stochastic Algorithm for Estimating Maximum-Likelihood Phylogenies. Molecular

540 Biology and Evolution 32:268–274.

541 49. Kalyaanamoorthy S, Minh BQ, Wong TKF, von Haeseler A, Jermiin LS. 2017.

542 ModelFinder: fast model selection for accurate phylogenetic estimates. Nat Methods 14:587–

543 589.

544 50. Kanehisa M. 2000. KEGG: Kyoto Encyclopedia of Genes and Genomes. Nucleic Acids

545 Research 28:27–30.

546 51. Galperin MY, Makarova KS, Wolf YI, Koonin EV. 2015. Expanded microbial genome

547 coverage and improved protein family annotation in the COG database. Nucleic Acids Research

548 43:D261–D269.

549 52. Mistry J, Chuguransky S, Williams L, Qureshi M, Salazar GA, Sonnhammer ELL,

bioRxiv preprint doi: https://doi.org/10.1101/2022.01.05.475171; this version posted January 7, 2022. The copyright holder for this preprint (which was not certified by peer review) is the author/funder, who has granted bioRxiv a license to display the preprint in perpetuity. It is made available under aCC-BY-ND 4.0 International license.

550 Tosatto SCE, Paladin L, Raj S, Richardson LJ, Finn RD, Bateman A. 2021. Pfam: The protein
551 families database in 2021. Nucleic Acids Research 49:D412–D419.
552 53. Weigel BL, Miranda KK, Fogarty EC, Watson AR, Pfister CA. in review. Functional
553 insights into the kelp microbiome from metagenome assembled genomes.
554 54. Letunic I, Bork P. 2021. Interactive Tree Of Life (iTOL) v5: an online tool for
555 phylogenetic tree display and annotation. Nucleic Acids Research 49:W293–W296.
556 55. Kapili BJ, Dekas AE. 2021. PPIT: an R package for inferring microbial taxonomy from
557 *nifH* sequences. Bioinformatics 37:2289–2298.
558 56. Shelton AO. 2010. Temperature and community consequences of the loss of foundation
559 species: Surfgrass (Phyllospadix spp., Hooker) in tidepools. Journal of Experimental Marine
560 Biology and Ecology 391:35–42.
561 57. Lefcheck JS, Wilcox DJ, Murphy RR, Marion SR, Orth RJ. 2017. Multiple stressors
562 threaten the imperiled coastal foundation species eelgrass (*Zostera marina*) in Chesapeake Bay,
563 USA. Glob Change Biol 23:3474–3483.
564 58. Pfister CA, Altabet MA, Weigel BL. 2019. Kelp beds and their local effects on seawater
565 chemistry, productivity, and microbial communities. Ecology https://doi.org/10.1002/ecy.2798.
566 59. Miranda KK, Weigel BL, McCoy SJ, Pfister CA. 2021. Differential impacts of alternate
567 primary producers on carbon cycling. Ecology https://doi.org/10.1002/ecy.3455.
568 60. Liggan LM, Martone PT. 2018. Under pressure: biomechanical limitations of developing
569 pneumatocysts in the bull kelp (*Nereocystis luetkeana* , Phaeophyceae). Journal of Phycology
570 54:608–615.
571 61. Egan S, Harder T, Burke C, Steinberg P, Kjelleberg S, Thomas T. 2013. The seaweed
572 holobiont: understanding seaweed–bacteria interactions. FEMS Microbiology Reviews 37:462–

bioRxiv preprint doi: https://doi.org/10.1101/2022.01.05.475171; this version posted January 7, 2022. The copyright holder for this preprint (which was not certified by peer review) is the author/funder, who has granted bioRxiv a license to display the preprint in perpetuity. It is made available under aCC-BY-ND 4.0 International license.

476.

62. Minich JJ, Morris MM, Brown M, Doane M, Edwards MS, Michael TP, Dinsdale EA. 2018. Elevated temperature drives kelp microbiome dysbiosis, while elevated carbon dioxide induces water microbiome disruption. PLOS ONE 13:e0192772.

63. Capistrant-Fossa KA, Morrison HG, Engelen AH, Quigley CTC, Morozov A, Serrão EA, Brodie J, Gachon CMM, Badis Y, Johnson LE, Hoarau G, Abreu MH, Tester PA, Stearns LA, Brawley SH. 2021. The microbiome of the habitat-forming brown alga *Fucus vesiculosus* (Phaeophyceae) has similar cross-Atlantic structure that reflects past and present drivers [1]. J Phycol jpy.13194.

64. Li J, Weinberger F, Saha M, Majzoub ME, Egan S. 2021. Cross-Host Protection of Marine Bacteria Against Macroalgal Disease. Microb Ecol https://doi.org/10.1007/s00248-021-01909-2.

65. Burgunter-Delamare B, KleinJan H, Frioux C, Fremy E, Wagner M, Corre E, Le Salver A, Leroux C, Leblanc C, Boyen C, Siegel A, Dittami SM. 2020. Metabolic Complementarity Between a Brown Alga and Associated Cultivable Bacteria Provide Indications of Beneficial Interactions. Front Mar Sci 7:85.

66. Mohr W, Lehnen N, Ahmerkamp S, Marchant HK, Graf JS, Tschitschko B, Yilmaz P, Littmann S, Gruber-Vodicka H, Leisch N, Weber M, Lott C, Schubert CJ, Milucka J, Kuypers MMM. 2021. Terrestrial-type nitrogen-fixing symbiosis between seagrass and a marine bacterium. Nature https://doi.org/10.1038/s41586-021-04063-4.

67. Noisette F, Hurd C. 2018. Abiotic and biotic interactions in the diffusive boundary layer of kelp blades create a potential refuge from ocean acidification. Functional Ecology 32:1329–1342.

bioRxiv preprint doi: https://doi.org/10.1101/2022.01.05.475171; this version posted January 7, 2022. The copyright holder for this preprint (which was not certified by peer review) is the author/funder, who has granted bioRxiv a license to display the preprint in perpetuity. It is made available under aCC-BY-ND 4.0 International license.

596 68. Weigel BL, Pfister CA. 2020. Oxygen metabolism shapes microbial settlement on
597 photosynthetic kelp blades compared to artificial kelp substrates. Environmental Microbiology
598 Reports 1758-2229.12923.
599 69. Moulton O, Hacker S. 2011. Congeneric variation in surfgrasses and ocean conditions
600 influence macroinvertebrate community structure. Mar Ecol Prog Ser 433:53–63.
601 70. Howarth RW, Hobbie JE. 1982. THE REGULATION OF DECOMPOSITION AND
602 HETEROTROPHIC MICROBIAL ACTIVITY IN SALT MARSH SOILS: A REVIEW, p. 183–
603 207. *In* Estuarine Comparisons. Elsevier.
604 71. Martin BC, Middleton JA, Fraser MW, Marshall IPG, Scholz VV, Hausl B, Schmidt H.
605 2020. Cutting out the middle clam: lucinid endosymbiotic bacteria are also associated with
606 seagrass roots worldwide. ISME J 14:2901–2905.
607 72. Keller AH, Schleinitz KM, Starke R, Bertilsson S, Vogt C, Kleinsteuber S. 2015.
608 Metagenome-Based Metabolic Reconstruction Reveals the Ecophysiological Function of
609 Epsilonproteobacteria in a Hydrocarbon-Contaminated Sulfidic Aquifer. Front Microbiol 6.
610 73. Helliwell KE. 2017. The roles of B vitamins in phytoplankton nutrition: new perspectives
611 and prospects. New Phytol 216:62–68.
612 74. Babbin AR, Tamasi T, Dumit D, Weber L, Rodríguez MVI, Schwartz SL, Armenteros M,
613 Wankel SD, Apprill A. 2021. Discovery and quantification of anaerobic nitrogen metabolisms
614 among oxygenated tropical Cuban stony corals. ISME J 15:1222–1235.
615 75. Fiore CL, Jarett JK, Olson ND, Lesser MP. 2010. Nitrogen fixation and nitrogen
616 transformations in marine symbioses. Trends in Microbiology 18:455–463.
617 76. Morris RL, Schmidt TM. 2013. Shallow breathing: bacterial life at low O2. Nature
618 Reviews Microbiology 11:205–212.

bioRxiv preprint doi: https://doi.org/10.1101/2022.01.05.475171; this version posted January 7, 2022. The copyright holder for this preprint (which was not certified by peer review) is the author/funder, who has granted bioRxiv a license to display the preprint in perpetuity. It is made available under aCC-BY-ND 4.0 International license.

619 77. Lilja EE, Johnson DR. 2019. Substrate cross-feeding affects the speed and trajectory of
620 molecular evolution within a synthetic microbial assemblage. BMC Evol Biol 19:129.
621 78. de Jesús Astacio LM, Prabhakara KH, Li Z, Mickalide H, Kuehn S. 2020. Closed
622 microbial communities self-organize to persistently cycle carbon. preprint, Ecology.
623 79. Goldford JE, Lu N, Bajić D, Estrela S, Tikhonov M, Sanchez-Gorostiaga A, Segrè D,
624 Mehta P, Sanchez A. 2018. Emergent simplicity in microbial community assembly. Science
625 361:469–474.
626 80. Hamersley MR, Sohm JA, Burns JA, Capone DG. 2015. Nitrogen fixation associated
627 with the decomposition of the giant kelp Macrocystis pyrifera. Aquatic Botany 125:57–63.
628 81. McGlathery K, Risgaard-Petersen N, Christensen P. 1998. Temporal and spatial variation
629 in nitrogen fixation activity in the eelgrass Zostera marina rhizosphere. Mar Ecol Prog Ser
630 168:245–258.
631 82. Garcias-Bonet N, Arrieta JM, Duarte CM, Marbà N. 2016. Nitrogen-fixing bacteria in
632 Mediterranean seagrass (Posidonia oceanica) roots. Aquatic Botany 131:57–60.
633 83. Steunou A-S, Jensen SI, Brecht E, Becraft ED, Bateson MM, Kilian O, Bhaya D, Ward
634 DM, Peters JW, Grossman AR, Kühl M. 2008. Regulation of nif gene expression and the
635 energetics of N2 fixation over the diel cycle in a hot spring microbial mat. ISME J 2:364–378.
636 84. Cardini U, van Hoytema N, Bednarz VN, Al-Rshaidat MMD, Wild C. 2018. N_2 fixation
637 and primary productivity in a red sea *Halophila stipulacea* meadow exposed to seasonality: N_2
638 *fixation in* Halophila stipulacea. Limnol Oceanogr 63:786–798.
639 85. Agawin NSR, Gil Atorrasagasti MG, Frank Comas A, Fernández-Juárez V, López-
640 Alforja X, Hendriks IE. 2021. Response of the seagrass *POSIDONIA OCEANICA* and its associated
641 N_2 fixers to high business-as-usual climate change scenario in winter. Limnol Oceanogr

bioRxiv preprint doi: https://doi.org/10.1101/2022.01.05.475171; this version posted January 7, 2022. The copyright holder for this preprint (which was not certified by peer review) is the author/funder, who has granted bioRxiv a license to display the preprint in perpetuity. It is made available under aCC-BY-ND 4.0 International license.

642 lno.11758.

643

644 Table 1. Summary of the features of 8 metagenomes. More information is in Table S1 and the

645 taxonomy based on single copy genes is in Table S2.

Phyllospadix scouleri			*Phyllospadix serrulatus*	*Laminaria setchellii*	*Nereocystis luetkeana*	*Zostera marina*	
Sediment	Rhizome	Blade	Rhizome	Blade	Inner bulb	Sediment	Rhizome
# quality reads (in millions)							
43.68	67.73	38.41	37.99	48.58	6.48	19.37	65.76
Bacteria							
63.7%	58.3%	63.6%	63.0%	63.9%	62.2%	33.6%	60.6%
Archaea							
34.2%	38.3%	33.1%	33.3%	32.7%	35.9%	62.1%	34.2%

646

647

bioRxiv preprint doi: https://doi.org/10.1101/2022.01.05.475171; this version posted January 7, 2022. The copyright holder for this preprint (which was not certified by peer review) is the author/funder, who has granted bioRxiv a license to display the preprint in perpetuity. It is made available under aCC-BY-ND 4.0 International license.

Table 2. Metagenome assembled genomes across all samples and their representation across phyla. More detailed information on the MAGs can be found in Table S3.

Phyllospadix scouleri			*Phyllospadix serrulatus*	*Laminaria setchellii*	*Nereocystis luetkeana*	*Zostera marina*	
Sediment	Rhizome	Blade	Rhizome	Blade	Inner bulb	Sediment	Rhizome
High Quality MAGs							
3	1	7	6	9	1	2	5
Other MAGs							
2	2	8	7	7	0	5	7
Proteobacteria							
2	-	9	2	10	1	5	5
Bacteroidota							
3	2	5	4	4	-	-	1
Verrucomicrobia							
-	-	-	-	2	-	-	-
Campylobacterota							
-	-	-	-	-	-	2	1
Desulfobacterota							
-	-	-	2	-	-	-	3
Desulfuromonadota							
-	-	-	1	-	-	-	-
Acidobacteriota							
-	-	-	1	-	-	-	-
Spirochaetota							
-	-	-	1	-	-	-	-
No ID							
-	-	1	2	-	-	-	2
Crenarchaeota							
-	1	-	-	-	-	-	-

bioRxiv preprint doi: https://doi.org/10.1101/2022.01.05.475171; this version posted January 7, 2022. The copyright holder for this preprint (which was not certified by peer review) is the author/funder, who has granted bioRxiv a license to display the preprint in perpetuity. It is made available under aCC-BY-ND 4.0 International license.

Figure Captions

Figure 1. Boxplot comparing the dissolved oxygen concentrations of water column (blue) and the sediment-rhizome environment (red) of *P. scouleri* (pairwise t-test: $p<0.001$) and *P. serrulatus* (pairwise t-test: $p<0.001$). Sampling dates are represented by different colors.

Figure 2. A phylogenomic tree of 6 concatenated bacterial single-copy core ribosomal genes from 71 bacterial MAGS across 8 samples, showing the results from 33 high quality MAGs and 38 lower quality ones. One MAG, PSC_RHZ_Bin_00003, from the rhizome of *P. scouleri*, was identified as an archaeal genome and was thus omitted from this tree. Gaps in class, family and genus indicate the level to which taxonomic classification was resolved in each MAG. All blade tissues have 'water column exposure', while rhizome and sediment samples do not.

Figure 3. Microbial Metabolisms in the MAGs reported in Fig. 2 and Table S3 across all hosts and grouped as those that might benefit the host ("hosts benefit") and microbial metabolisms that might utilize host provisioned metabolites ("microbes benefit"). Each tick along the x-axis corresponds to a MAG. *N. luetkeana* blade MAGs are from Weigel et al. (in review). The metabolisms for **DOC Uptake** that benefit microbes are shown as a heatmap of the count of the number of genes that can metabolize *Compatible Solutes*, *Carboxylic Acids*, *Carbohydrate Pentoses* and *General Carbohydrates*. Microbial metabolisms that benefit the host are **Ammonification Hydrolases,** where the heatmap provides a count of the hydrolases acting on C-N bonds other than peptide bonds, **Nitrogen Metabolisms** and **Vitamin** Synthesis, both shown as the presence or absence of a gene in a pathway. The genes used in this are in Table S4.

bioRxiv preprint doi: https://doi.org/10.1101/2022.01.05.475171; this version posted January 7, 2022. The copyright holder for this preprint (which was not certified by peer review) is the author/funder, who has granted bioRxiv a license to display the preprint in perpetuity. It is made available under aCC-BY-ND 4.0 International license.

675 **Figure 4**. A phylogenomic tree of *nifH* genes found on the rhizomes of *P. serrulatus* (PSE,
676 n = 3) and the rhizomes and surrounding sediment of *Z. marina* (ZMA, n = 2 and 5,
677 respectively). Some *nifH* genes group into Cluster I, including a sulfur oxidizing taxon on the
678 rhizome of *Z. marina*, and other taxa in *Campylobacterota*, including *Sulfurovum*. Cluster III
679 contains taxa associated with rhizomes including rhizomes including *Desulfobulbus*
680 *mediterraneus* on *P. serrulatus* and a Desulfobacterales associated with *Z. marina* rhizomes.
681

bioRxiv preprint doi: https://doi.org/10.1101/2022.01.05.475171; this version posted January 7, 2022. The copyright holder for this preprint (which was not certified by peer review) is the author/funder, who has granted bioRxiv a license to display the preprint in perpetuity. It is made available under aCC-BY-ND 4.0 International license.

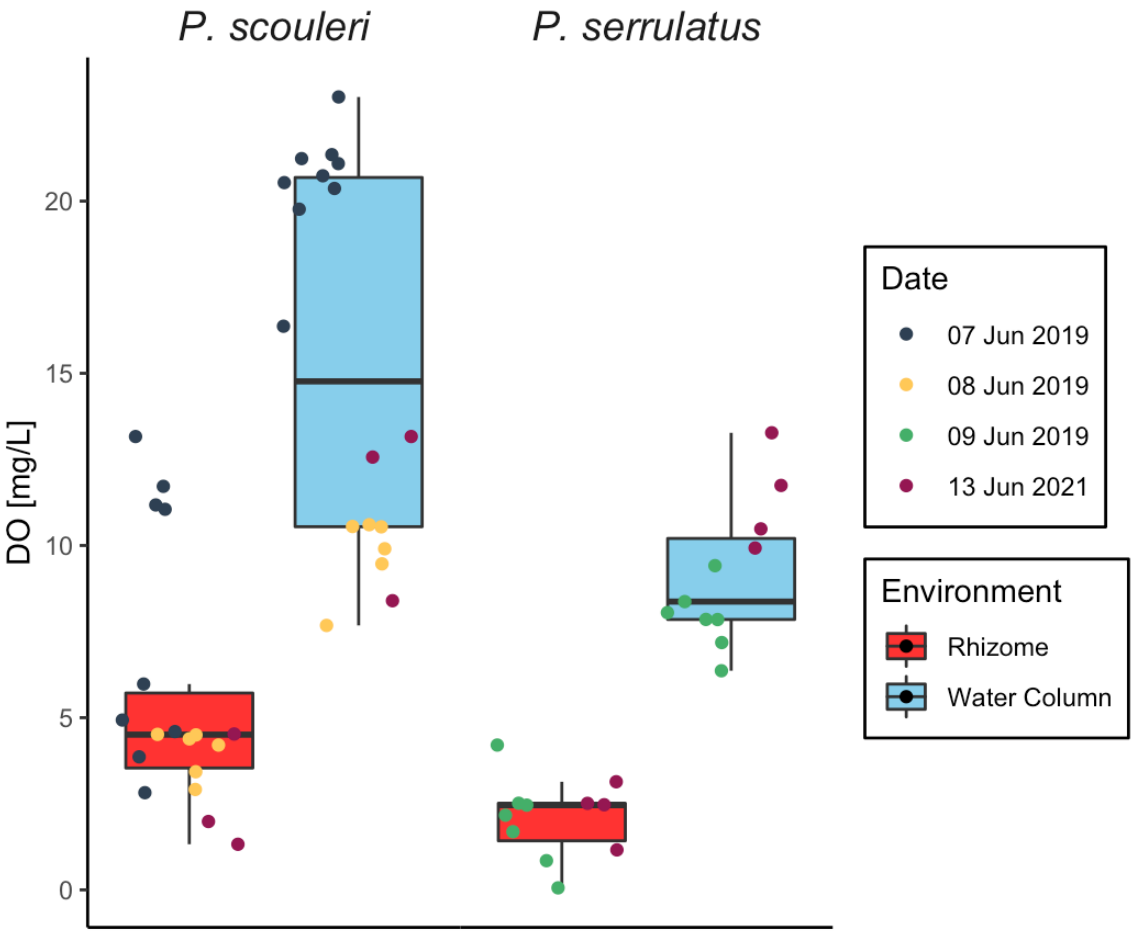

682

683 **Figure 1**

bioRxiv preprint doi: https://doi.org/10.1101/2022.01.05.475171; this version posted January 7, 2022. The copyright holder for this preprint (which was not certified by peer review) is the author/funder, who has granted bioRxiv a license to display the preprint in perpetuity. It is made available under aCC-BY-ND 4.0 International license.

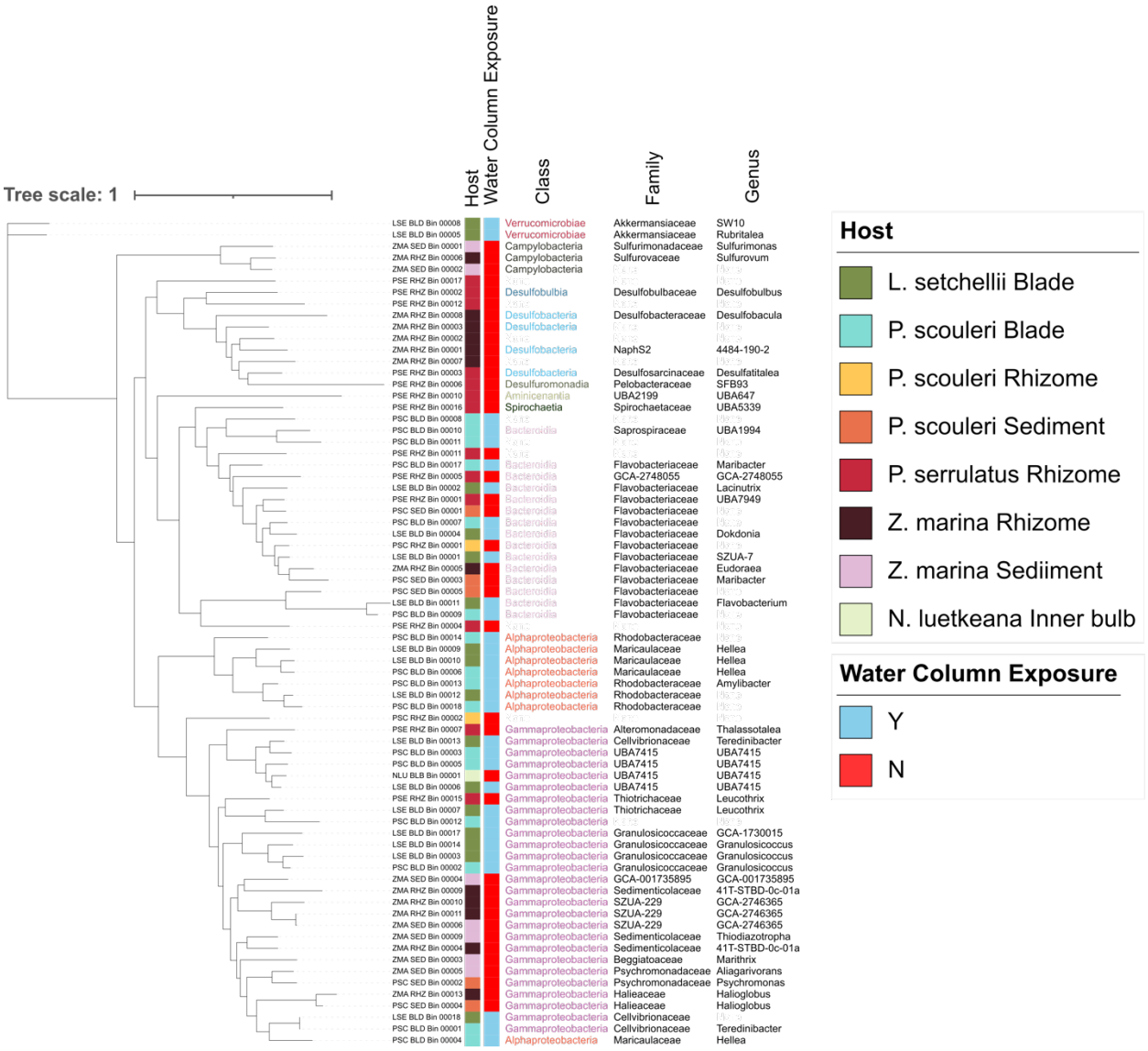

Figure 2

bioRxiv preprint doi: https://doi.org/10.1101/2022.01.05.475171; this version posted January 7, 2022. The copyright holder for this preprint (which was not certified by peer review) is the author/funder, who has granted bioRxiv a license to display the preprint in perpetuity. It is made available under aCC-BY-ND 4.0 International license.

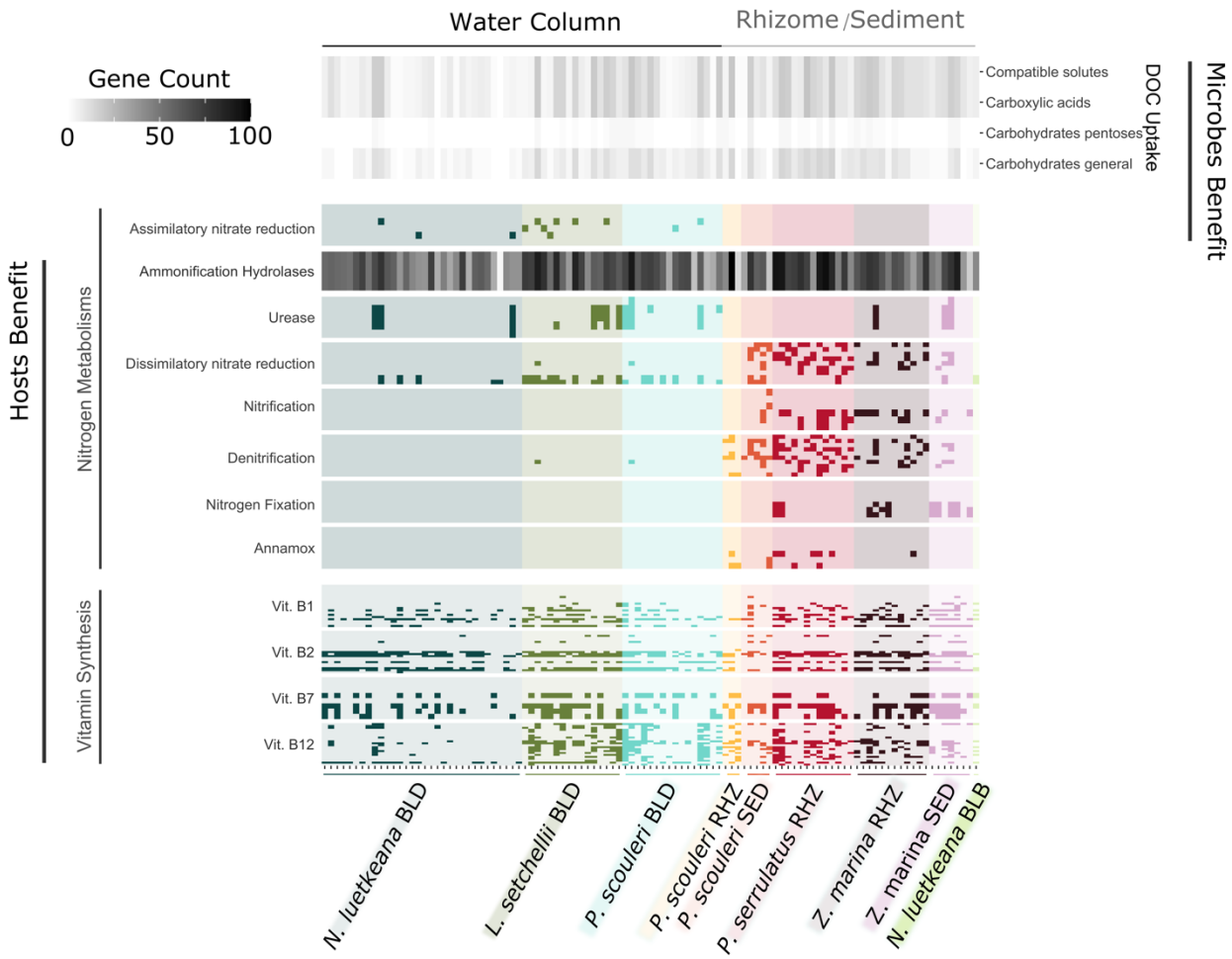

Figure 3

bioRxiv preprint doi: https://doi.org/10.1101/2022.01.05.475171; this version posted January 7, 2022. The copyright holder for this preprint (which was not certified by peer review) is the author/funder, who has granted bioRxiv a license to display the preprint in perpetuity. It is made available under aCC-BY-ND 4.0 International license.

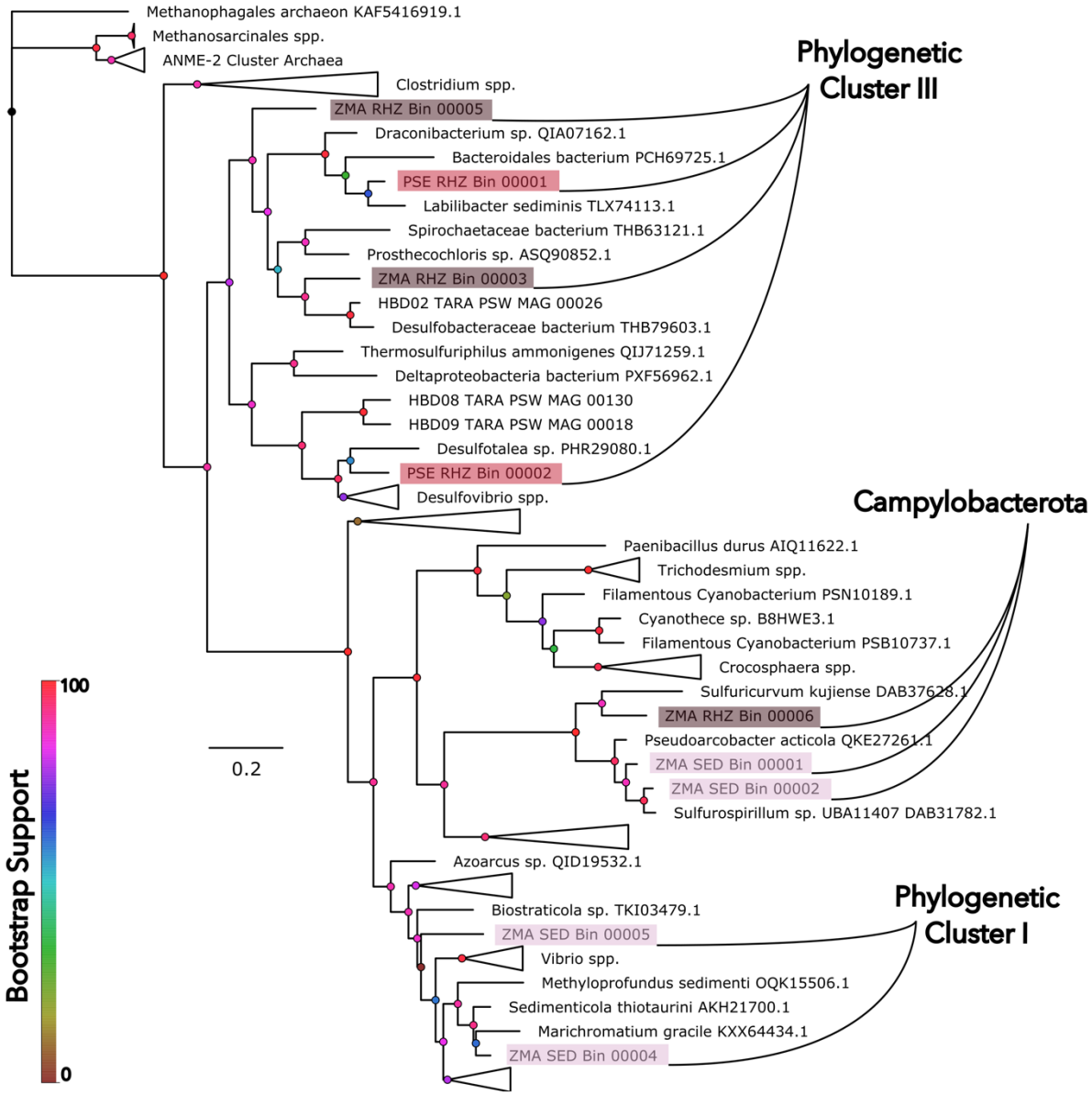

Figure 4

bioRxiv preprint doi: https://doi.org/10.1101/2022.01.05.475171; this version posted January 7, 2022. The copyright holder for this preprint (which was not certified by peer review) is the author/funder, who has granted bioRxiv a license to display the preprint in perpetuity. It is made available under aCC-BY-ND 4.0 International license.

691 **Supplementary Files**

692 **Table S1**. A summary of eight metagenomes from five macrophyte taxa.

693 **Table S2**. A summary of taxonomy of MAGs

694 **Table S3**. The features of 72 metagenome assembled genomes (MAGs).

695 **Table S4**. Genes used to generate Fig. 3

696 **Table S5**. The features of *nifH* genes found in MAGs.

697 **Table S6**. *nifH* reference amino acid sequences

698

699 **Appendix 1.** Additional methods to quantify carbon and nitrogen stable isotopes in *P. scouleri*

700 **Figure S1**. Stable isotope analysis of delC13 and delN15 at blade tip, meristem, rhizome of P.

701 scouleri. From blade tip to rhizome, water flow and thus elemental mixing reduces due to

702 attenuation and boundary layer effects of surfgrass canopy. Assuming elemental uptake occurs

703 from the same pools of C and N, the lower the extent of mixing, the heavier the isotopic

704 signature should be at that point of the plant. This is observed with delC13 which gets heavier

705 from the tip to the blade. This is observed with delN15 till the meristem after which it lightens.

706 This is probably occurring as nitrogen is taken up from a different pool of nitrogen from that

707 around the blade/meristem. This different pool is probably made available through n-fixation